Published in final edited form as:
Curr Biol. 2015 January 19; 25(2): 218–224. doi:10.1016/j.cub.2014.11.017.

Dynamic visualization of α-catenin reveals rapid, reversible conformation switching between tension states

Tae-Jin Kim[1], **Shuai Zheng**[2], **Jie Sun**[3], **Ismaeel Muhamed**[4], **Jun Wu**[5], **Lei Lei**[6], **Xinyu Kong**[4], **Deborah E. Leckband**[2,4,5,6,7,8,*], and **Yingxiao Wang**[1,2,3,6,8,9,*]

[1]Neuroscience Program, University of Illinois, Urbana-Champaign, Urbana, IL 61801, USA

[2]Department of Bioengineering & Beckman Institute for Advanced Science and Technology, University of Illinois, Urbana-Champaign, Urbana, IL 61801, USA

[3]Department of Integrative and Molecular Physiology, University of Illinois, Urbana-Champaign, Urbana, IL 61801, USA

[4]Department of Biochemistry, University of Illinois, Urbana-Champaign, Urbana, IL 61801, USA

[5]Department of Chemical and Biomolecular Engineering, University of Illinois, Urbana-Champaign, Urbana, IL 61801, USA

[6]Center for Biophysics and Computational Biology, University of Illinois, Urbana-Champaign, Urbana, IL 61801, USA

[7]Department of Chemistry, University of Illinois, Urbana-Champaign, Urbana, IL 61801, USA

[8]Institute for Genomic Biology, University of Illinois, Urbana-Champaign, Urbana, IL 61801, USA

[9]Department of Bioengineering and Institute of Engineering in Medicine, University of California, San Diego, La Jolla, CA 92093, USA

Summary

The cytosolic protein α–catenin is a postulated force-transducer at cadherin complexes [1]. The demonstration of force activation, identification of consequent downstream events in live cells,

*Address correspondence to these authors. Deborah E. Leckband, Ph.D., Department of Chemical and Biomolecular Engineering, Department of Chemistry, Tel: +1-217-244-0793, Fax: +1-217-333-5052, leckband@illinois.edu. Yingxiao Wang, Ph.D., Department of Bioengineering, University of California, San Diego, CA 92093, Tel: +1-858-822-4502, yiw015@eng.ucsd.edu.

Conflict of Interest Disclosure Statement
The authors declare no competing financial interests.

Author contributions
T.K.: conception and design, experiments, data analysis and interpretation, manuscript writing, final approval of manuscript; S.Z.: conception and design, experiments, manuscript writing; J.S.: conception and design, experiments; L.L., J.W., X.K., and I.M.: conception and experiments; D.E.L and Y.W.; conception and design, data analysis and interpretation, manuscript writing, final approval of manuscript

Supplementary information
Supplemental information includes four figures and Supplementary Experimental Procedures

and development of tools to study these dynamic processes in living cells are central to elucidating the role of α–catenin in cellular mechanics and tissue function [2–10]. Here we demonstrate that α–catenin is a force-activatable mechano-transducer at cell-cell junctions, using an engineered α-catenin conformation sensor, based on fluorescence resonance energy transfer (FRET). This sensor reconstitutes α-catenin-dependent functions in α-catenin depleted cells, and recapitulates the behavior of the endogenous protein. Dynamic imaging of cells expressing the sensor demonstrated that α-catenin undergoes immediate, reversible conformational switching, in direct response to different mechanical perturbations of cadherin adhesions. Combined magnetic twisting cytometry with dynamic FRET imaging [11] revealed rapid, local conformational switching, upon the mechanical stimulation of specific cadherin bonds. At acutely stretched cell-cell junctions, the immediate, reversible conformational change further reveals that α-catenin behaves like an elastic spring in series with cadherin and actin. The force-dependent recruitment of vinculin—a principal α-catenin effector—to junctions requires the vinculin-binding-site of the α–catenin sensor [1, 12–16]. In cells, the relative rates of force-dependent α–catenin conformation switching and vinculin recruitment reveal that α–catenin activation and vinculin recruitment occur sequentially rather than in a concerted process, with vinculin accumulation being significantly slower. This engineered α-catenin sensor revealed that α–catenin is a reversible, stretch-activatable sensor that mechanically links cadherin complexes and actin, and is an indispensable player in cadherin-specific mechano-transduction at intercellular junctions.

Keywords

FRET biosensor; Live-cell Imaging; α-catenin; Mechano-transduction; Cadherin; Cell-Cell Junction

Results and Discussion

α-catenin FRET sensor localizes to intercellular junctions and restores α-catenin dependent functions in α-catenin depleted cells

We generated an α–catenin conformation sensor, by inserting fluorescent proteins, ECFP and YPet into flexible linkers flanking the central, proposed force sensing α-catenin module (D2–D4, Fig. 1A). Western blots (Fig. S1A) and fluorescence images (Fig. S1B) verified the sensor expression and localization in transfected, α–catenin-knock-down MDCK cells (MDCK KD) and in MDCK WT cells (Fig. S1B). In Western blots, the faint sensor band relative to endogenous α-catenin (Fig. S1A) is attributed to the low sensor transfection efficiency. The biosensor localizes to intercellular junctions when expressed in either MDCK WT cells or in MDCK KD cells, and it co-localizes with endogenous α-catenin (Fig. S1B). The sensor similarly localized to junctions between transfected, α-catenin deficient R2/7 cells (see Fig. 1C, Fig. S1E).

The sensor is overexpressed in DLD1 and MDCK epithelial cells, but prior findings demonstrated that α–catenin-GFP overexpression in DLD1-R2/7 cells [15, 16] or in MDCK KD cells [16] did not affect cadherin-based mechanotransduction, vinculin and actin recruitment, or traction force generation [16]. Nor did cytosolic α–catenin depletion alter cadherin-based mechanotransduction [16].

The sensor expression restored α-catenin-dependent adhesive functions in α-catenin-deficient MDCK KD and DLD-1 R2/7 cells. A signature of force-transducers at cell adhesions is their ability to alter receptor-mediated spreading and traction force generation, in response to substrate rigidity (Fig. S1C) [16–18]. The sensor expression restored traction forces exerted by MDCK KD cells to MDCK WT levels (Fig. S1D). Traction measurements were conducted in medium containing 0.5% FBS and anti-α_v and β_6 integrin antibodies GOH3 and AIIB2, in order to block integrin interference.

Cells exert greater traction forces on E-Cadherin adhesions on rigid versus soft substrates [16, 17]. According to the sensor design (Fig. 1A), the increased tension on cadherin adhesions would stretch α-catenin, separate YPet from ECFP, and decrease the FRET/ECFP ratio. Consistent with a tension-dependent change in conformation, the basal FRET/ECFP ratios measured with DLD1-R2/7 cells expressing the α–catenin sensor were lower in cells adhered to more rigid (40 kPa modulus) E-cadherin-coated gels than in cells on softer gels (0.6 kPa modulus) (Figs. S1E,F). Together, these findings demonstrate that the engineered α–catenin FRET sensor localizes to intercellular junctions, and rescues α-catenin-dependent adhesion, traction generation, and rigidity sensing at E-cadherin adhesions.

Altered junctional tension triggers α–catenin conformational switching

Altered physiological levels of tension across cadherin junctions were predicted to induce corresponding changes in dynamic FRET signals at different subcellular locations, and would allow the mapping of spatiotemporal activation patterns of α-catenin in cells. Three methods were used to disrupt mechanical coupling between cadherin bonds and F-actin (Figs. 1C,D&S2). Both disrupting cadherin bonds with E-cadherin blocking antibody DECMA-1 (Figs. 1C,D) [19] and removing Ca^{2+} (Figs. S2A,B) inactivates cadherin adhesion and lowers intercellular tension [20]. Actin disruption with cytochalasin D (CytoD) (Fig. S2C–F) also destabilizes junctions and reduces tension [20, 21].

The observed increase in the FRET/ECFP ratio at regions of interest (ROI) at cell junctions following junction disruption with inactivating antibody (Fig. 1C,D) indicates a corresponding switch to the relaxed sensor conformation (Fig. 1A, right). Results with a neutral, anti-E-cadherin antibody confirmed that cadherin inactivation caused the FRET/ECFP change (Fig. 1D). At physiological Ca^{2+} concentrations (2mM), the average FRET/ECFP ratio in ROIs at junctions between DLD-1 R2/7 cells expressing the sensor was lower than between cells following Ca^{2+} removal (Figs. S2A,B). The overall signal increase was complete within 2 min of Ca^{2+} removal, and occurred well before the appearance of visible intercellular gaps. In studies with MDCK KD cells expressing the sensor, calcium removal also increased the FRET/ECFP ratio from 1.74 ± 0.03 to 2.04 ± 0.04 (n=11, $P < 0.01$) (data not shown).

Actin disruption with Cyto D increased the FRET/ECFP ratio by ~7%, relative to untreated DLD1-R/27 cells (Figs. S2C,D). With transfected MDCK KD cells expressing the sensor, CytoD treatment similarly increased the FRET/ECFP ratio at junctions from 1.67 ± 0.03 to 1.78 ± 0.04 (n=14, $P < 0.01$) (data not shown). This visualized tension-dependent conformational change occurred in the presence of endogenous α–catenin. At junctions between transfected MDCK WT cells, the FRET/ECFP ratio increased following CytoD

treatment (Fig. S2E,F). Changes in the cytosolic FRET/ECFP ratios were negligible (Fig. S2F).

The tension-dependent conformational switch does not require the vinculin-binding-site (VBS), which is required for vinculin recruitment and local cytoskeletal remodeling [1, 9, 14, 16]. The α–Cat-ΔVBS-sensor, in which the VBS was replaced with the homologous vinculin sequence [1, 15, 16](Fig. 1B), retained the F-actin and β–catenin binding sites and localized to junctions (Figs. S3A). CytoD treatment increased the FRET/ECFP ratio in DLD1-R2/7 cells expressing this mutant sensor, demonstrating that the vinculin site is not required for force-dependent conformation switching (Figs. S3A,B).

Cytosolic α–catenin dimers do not contribute to tension-dependent FRET changes

To test whether dimers of the cytosolic α-catenin sensor [22] contribute to changes in force-dependent FRET/ECFP ratios, control constructs were engineered with point mutations that quenched either the ECFP or the YPet fluorescence (Fig. 1B). The 67G>A substitution in YPet in the "α-catenin-ECFP" construct quenched YPet fluorescence, and the double mutant 66W>A, 67G>A in ECFP quenched ECFP fluorescence in the "α-catenin-YPet" construct [23, 24]. In both cases, the second fluorophore and the α-catenin core were unaffected (Fig. S4A), and both mutants localized to junctions.

In MDCK WT cells co-transfected with both fluorophore mutants, Cyto D treatment did not detectably alter the cytosolic or junctional FRET/ECFP ratio (Figs. S4B,C). By comparison, the FRET/ECFP ratio in ROIs between MDCK WT cells expressing the WT α-Cat sensor increased by ~4%, after actin disruption (Fig. S4B,C). In MDCK WT cells expressing the WT α–Cat sensor, FRET/ECFP ratios in ROIs at junctions versus the cytosol also confirmed that cytosolic dimers do not undergo tension-dependent conformation changes (Fig. S2F).

Cadherin-specific receptor loading triggers an immediate α-catenin conformational switch with consequent vinculin recruitment

Cadherin-based mechanotransduction has been investigated by dynamically twisting E-cadherin-coated, ferromagnetic beads bound to E-cadherin receptors at the cell surface (Fig. 2A)[16, 21, 25]. Combined magnetic twisting cytometry (MTC) and dynamic fluorescence imaging established spatiotemporal correlations between dynamic E-cadherin loading, α-catenin conformation switching, and vinculin recruitment. Prior to twisting E-cadherin-Fc-coated beads attached to transiently transfected MDCK WT cells, the FRET/ECFP ratio in the ROI surrounding the beads (Fig. 2C) was stable, but decreased following bond shear (Fig. 2B). The decreasing trend in the FRET/ECFP ratio was apparent within 1.5s of data acquisition, and the difference was statistically significant at 4.5s. Subsequent fluorescent images were acquired every 0.5s, although Fig. 2B reports the FRET/ECFP ratios at 1.5s intervals. This rapid response is characteristic of mechanical activation [26, 27].

Within 2 min of force loading, vinculin accumulation was apparent around E-Cad-Fc beads on MDCK WT cells expressing the sensor (Fig. 2C,D). The force-dependent conformational switch and coincident vinculin recruitment was E-cadherin specific: twisting control, PLL (poly-L-lysine) beads neither changed the FRET/ECFP ratio at beads (PLL-bead, n=4 *versus*

E-Cad-bead, n=8, *P<0.05) (Fig. 2D) nor triggered vinculin recruitment (Fig. 2C,D, n=21–24, E-Cad-bead versus PLL-bead, ***P<0.001). These results agree with reports of MDCK KD and DLD1-R2/7 cells rescued with WT α-catenin-GFP [16].

The GFP expressed in MDCK KD cells as a knock down reporter [28] interferes with sensor imaging (particularly YPet signals) in MTC/FRET measurements. To establish whether the sensor recruits vinculin in a force-dependent manner that requires the vinculin-binding-site (VBS), studies instead used DLD1-R2/7 cells transfected with the WT sensor or the α–CatΔVBS sensor, which lacks the VBS (Fig. 1B). More vinculin accumulated at sheared E-Cad-Fc beads bound to DLD1-R2/7 cells expressing the WT α–Cat sensor (n=28–36, ***P<0.001) than to cells expressing the α–Cat-ΔVBS mutant (Figs. 2E,F). CytoD treatment ablated the force-dependent vinculin accumulation at E-Cad-beads on DLD1-R2/7 cells expressing the sensor (n=24–36, ***P<0.001) (Fig. 2F). These combined MTC/FRET measurements thus demonstrate that the α-catenin sensor undergoes a rapid conformational change in response to E-cadherin-specific, mechanical perturbations, and both the sensor and WT α–catenin require the VBS for force-dependent vinculin recruitment [1, 14–16].

Acute external stretch triggers conformational switching in the full-length α-catenin sensor

In combined MTC/FRET studies, the decrease in the FRET/ECFP ratio during continuous bead twisting could be due to slower adaptive biochemical signals or to accumulating stretched α-catenin conformers. We tested this by imaging dynamic FRET/ECFP changes at junctions between MDCK WT cells expressing the sensor (Fig. 3B), after applying an abrupt step change in junctional tension, using a nanoprobe that stretched the elastomeric cell substrates (Fig. 3A). Pressing the probe tip into exposed hydrogel adjacent to cells avoided direct contact with cells. Upon substrate stretch, the FRET/ECFP ratio at junctions decreased abruptly by ~4% to a stable level (Figs. 3B,C), without further adaptation. After tension release, the signal recoiled immediately to the initial value, with no hysteresis. In these measurements, 3 seconds was the shortest interval between stretching and FRET imaging (Fig. 3C). Measurements at 10s intervals gave similar results (Fig. S4D). Pretreatment with $GdCl_3$ prior to stretch-loading had no effect, and ruled out contributions from stretch-activated Ca^{2+} channels (not shown). Cadherin inactivation with blocking DECMA-1 antibody ablated the response (Fig. 3D). This immediate, reversible switching suggests that α-catenin functions like an elastic “spring” in series with the cytoskeleton, which deforms with the extracellular matrix and substrate. Comparison of the nanoprobe and MTC measurements indicates that the FRET/ECFP decrease during bead twisting (Fig. 2B) is due to continuous, mechanical perturbation rather than biochemical adaptation.

Biochemical signals during the 3s interval between substrate stretch and imaging could alter α–catenin. However, the rapid, reversible conformational switching without hysteresis (Figs. 3C & S4D) is a signature of mechanical activation, and is distinct from slower, dissipative biochemical reactions [26, 27]. By comparison, in PECAM-1 mechanotransduction studies, force-activated adaptive stiffening involves biochemical-signaling cascades. Adaptive stiffening had not stabilized 5s after initial PECAM-1 bead pulls [29]. After releasing tension, a much slower relaxation back to the initial state exhibited hysteresis typical of

dissipative biochemical processes [29]. Consequently, the observed rapid, reversible, mechanically triggered conformational switching supports a model in which α-catenin functions as a reversible, elastic force transducer in series with cadherin and actin. Mechanically induced α–catenin unfolding was demonstrated in vitro [30], but these results reveal force actuated, reversible conformational switching and the associated dynamics in live cells. The rapid mechanical response and studies with domain deletion mutants also supports mechanical connectivity between cadherin, α-catenin and the cytoskeleton.

Studies with two sensor mutants lacking either residues 48–163 or residues 849–906 (Fig. 1B) demonstrated that sensor localization to cadherin complexes is required for conformation switching. These deletions removed the β-catenin (Δβ-catenin) or F-actin (ΔF-actin) binding sites, respectively. The Δβ-catenin mutant cannot bind the cadherin/β-catenin complex, and did not localize to junctions (Fig. S4E). Consistent with previous reports [14, 31, 32], the ΔF-actin mutant also remained in the cytoplasm, without clear junctional localization (Fig. S4E). The latter behavior may be due to the adoption of a conformation that allosterically impedes binding to β-catenin at junctions [14, 33]. In MDCK WT cells, neither of these constructs exhibited stretch-dependent changes in FRET/ECFP ratios, either at junctions or in the cytosol (Fig. S.4F). Cyto D treatment also did not alter FRET signals, in MDCK KD cells expressing either of these truncated sensors (Figs. S4E,F).

Force-activated vinculin recruitment to intercellular junctions lags α-catenin conformation switching

The dynamics of α-catenin conformational switching and vinculin recruitment in live cells were quantified during junction recovery, after a calcium switch. In line-scans of cell-cell junctions (Figs. 4A,B) one hour after re-activating cadherins with 2mM Ca^{2+}, the YPet intensity increased due to sensor accumulation at the re-annealing junctions (Figs. 4A,B). This coincided with a temporal decrease in FRET/ECFP ratios at junctions (Figs. 4C,D). There was no change in control cells without Ca^{2+} (Figs. 4A–D). The α-catenin conformation switching dynamics were slower during junction recovery (Figs. 4C,E) than following Ca^{2+} removal (Fig. S2B). The switching rate during junction recovery, estimated from a weighted nonlinear least squares fit of the FRET/ECFP decay (Fig. 4E) to a first order rate equation (Supplementary Information), was $0.15 \pm 0.06\ min^{-1}$.

The postulated vinculin co-activation by α-catenin and actin [34] suggested that α-catenin conformational switching might precede force-dependent vinculin accumulation at junctions. Immunofluorescence imaging showed that vinculin accumulates at re-annealing adhesions after Ca^{2+} activation [21]. Figure 4E shows the vinculin recruitment dynamics, quantified from fluorescence images of mCherry vinculin in ROIs at re-annealing junctions. The FRET/ECFP ratio decreased to the near steady-state level within 15 min (n=9–10, **P<0.01, relative to control) (Fig. 4C), but vincullin accumulated more slowly, during the 60 min observation period (n=32–36, **P<0.01) (Fig. 4E). The accumulation rate, estimated by fitting the vinculin accumulation time course (Fig. 4E) to pseudo first-order kinetics, was $0.025 \pm .002\ min^{-1}$. Immunofluorescence imaging (Fig. S3C) gave similar results: $0.017 \pm 0.004\ min^{-1}$. Thus, vinculin recruitment continues long after the α-catenin conformation reaches steady state at resealing junctions (Fig. 4E), and after 2min of E-

cadherin-bead twisting (not shown). Although vinculin could also bind β–catenin [35], it did not accumulate at re-annealing junctions between DLD1-R2/7 cells expressing the α–Cat-ΔVBS-GFP sensor (Fig. S3C). Therefore, in cells used in this study, vinculin accumulation requires α–catenin and its vinculin-binding-site, and the kinetics reflect vinculin recruitment to activated α–catenin. Whether vinculin recruitment also requires F-actin binding remains to be established.

Comparison of the recruitment dynamics of vinculin with mCherry labeled, constitutively active vinculin head domain (VH, residues 1–881) (Fig. 4F) demonstrated that the slow vinculin accumulation kinetics is due to its slow auto-inhibition release [36]. The fitted mCherry VH accumulation rate of 0.06 ± 0.01 min^{-1} was 3.5 fold faster than that of full-length mCherry VN. Although the mCherry VH expression was slightly higher than mCherry VN, it would need to be at least four times higher, in order for concentration differences to account for the different kinetics. Similarly, despite the immediate α–catenin conformational switch at junctions between briefly stretched (< 2min) MDCK monolayers, mCherry VH accumulation was slower, requiring several minutes of sustained stretch before statistically significant increases in mCherry VH were detected (Fig. S3D). Once docked, mCherry VH was retained for at least 10min after tension release (Figs. S3D,E). The slow release is consistent with the 98 ± 19nM dissociation constant between α–catenin and the vinculin head domain [37] that could kinetically stabilize the complex. Together, these findings directly demonstrate that, in live cells, the force-activation of α–catenin and vinculin recruitment occur sequentially, rather than by a concerted mechanism.

In summary, our engineered FRET-based α-catenin conformation sensor localizes to cadherin complexes at intercellular junctions and restores α–catenin dependent adhesive functions. This sensor undergoes immediate, reversible α–catenin conformational switching at cadherin adhesions, in response to mechanical perturbations. These results support the postulate α–catenin is an elastic, mechanically activated force transducer in series with cadherin and the cytoskeleton [1]. Kinetic analyses of coordinated conformation switching dynamics and vinculin recruitment further exposed molecular cascades in cadherin-based force transduction. Future comparisons of α-catenin sensor dynamics with force-dependent biochemical changes will uniquely reveal coordinated mechanical and biochemical events during mechanotransduction in live cells, with high spatiotemporal resolution.

Experimental Procedures

Complete experimental procedures are provided in Supplementary Experimental Procedures.

Reagents and Cells

The α–catenin conformation sensor was engineered by inserting the ECFP and acceptor YPet at the N- and C-terminal regions flanking the central force-sensing core of α–catenin (domains D2–D4). Five additional mutants were engineered for controls.

The following cell types were transiently transfected with the α–catenin sensor or its mutants: wild type Madine Darby canine kidney (MDCK WT) cells, an α–catenin

knockdown MDCK line (MDCK KD, gift from J. Nelson, Stanford [28]), DLD1 cells, and DLD1-R2/7, which is an α–catenin null subclone of the DLD1 line [38].

Vinculin recruitment was visualized with mCherry-vinculin (mCherry VN; from J. de Rooij, Utrecht) or by immunofluorescence imaging. Constitutively active mCherry (mCherry-VH, 1-881) was engineered as described in the Supplementary Experimental Methods.

Junction disruption

Tension across cadherin-based cell-cell junctions was disrupted by treating cells with the cadherin blocking antibody DECMA-1, by inactivating cadherin by Ca^{2+} depletion, or by disrupting actin with cytochalasin D treatment.

Junction reannealing after calcium switching

The addition of 2mM calcium, after junction disruption, activated cadherins and the subsequent restoration of cell-cell adhesions and junctional tension.

Time Lapse Live-Cell Imaging

Live-cell fluorescent images were obtained with a Zeiss Axiovert 200 inverted microscope and MetaFluor 6.2 software (Universal Imaging, West Chester, PA). The emission ratios of YPet/ECFP (referred to as the FRET/ECFP ratio) were directly computed using MetaFluor software, and analyzed further with Excel (Microsoft, Redmond, WA). During junction recovery assays, images were acquired with a Nikon fluorescence microscope with a Perfect Focus System (PFS), and image acquisition and analysis used MetaFluor 7.6 software.

Combined Magnetic Twisting Cytometry (MTC) and FRET

Magnetic beads coated with E-cadherin extracellular domains attached to cadherin receptors on the cell surface. An oscillating magnetic field twists the beads, to generate shear stress on E-cadherin bonds. FRET/ECFP ratios in regions of interest around the sheared beads (combined MTC/FRET) visualized force-activated changes in the sensor conformation triggered by mechanically perturbing specific E-cadherin bonds.

Substrate stretching measurements

Cells were cultured on an elastomeric substrate, and a nanoprobe was pressed into the substrate near the cells (Fig. 3A). Tangentially pulling the probe stretched the substrate, together with the extracellular matrix and attached cells to increase tension across the cell-cell contacts.

Statistical analysis

The fluorescence imaging and traction force results were expressed as the mean and standard error of the mean (S.E.M). The statistical significance of differences between two mean values was assessed using a Welch’s t-test or ANOVA supported by GraphPad Prism 6.0 Software. A statistically significant difference at the 95% confidence level is defined by a P value <0.05.

Supplementary Material

Refer to Web version on PubMed Central for supplementary material.

Acknowledgments

This work was supported in part by grants from NIH HL098472, HL109142, NSF CBET 08-46429 (YW), NIH R01 GM097443 (DEL), NSF CBET 11-32116 (DEL, YW).

References

1. Yonemura S, Wada Y, Watanabe T, Nagafuchi A, Shibata M. alpha-Catenin as a tension transducer that induces adherens junction development. Nat Cell Biol. 2010; 12:533–542. [PubMed: 20453849]
2. Lecuit T, Lenne PF, Munro E. Force Generation, Transmission, and Integration during Cell and Tissue Morphogenesis. Ann Rev Cell Dev Biol. 2011; 27:157–184. [PubMed: 21740231]
3. Huveneers S, de Rooij J. Mechanosensitive systems at the cadherin-F-actin interface. J Cell Sci. 2013; 126:403–413. [PubMed: 23524998]
4. Leckband D, de Rooij J. Cadherin adhesion and mechanosensing. Ann Rev Cell Develop Biol. 2014 in press.
5. Rauzi M, Lenne PF, Lecuit T. Planar polarized actomyosin contractile flows control epithelial junction remodelling. Nature. 2010; 468:1110–1114. [PubMed: 21068726]
6. Diz-Munoz A, Krieg M, Bergert M, Ibarlucea-Benitez I, Muller DJ, Paluch E, Heisenberg CP. Control of directed cell migration in vivo by membrane-to-cortex attachment. PLoS Biology. 2010; 8:e1000544. [PubMed: 21151339]
7. Papusheva E, Heisenberg CP. Spatial organization of adhesion: force-dependent regulation and function in tissue morphogenesis. EMBO J. 2010; 29:2753–2768. [PubMed: 20717145]
8. Maitre JL, Berthoumieux H, Krens SF, Salbreux G, Julicher F, Paluch E, Heisenberg CP. Adhesion functions in cell sorting by mechanically coupling the cortices of adhering cells. Science. 2012; 338:253–256. [PubMed: 22923438]
9. Leerberg JM, Gomez GA, Verma S, Moussa EJ, Wu SK, Priya R, Hoffman BD, Grashoff C, Schwartz MA, Yap AS. Tension-sensitive actin assembly supports contractility at the epithelial zonula adherens. Curr Biol. 2014; 24:1689–1699. [PubMed: 25065757]
10. Fernandez-Gonzalez R, de Simoes SM, Roper JC, Eaton S, Zallen JA. Myosin II dynamics are regulated by tension in intercalating cells. Dev Cell. 2009; 17:736–743. [PubMed: 19879198]
11. Na S, Wang N. Application of fluorescence resonance energy transfer and magnetic twisting cytometry to quantify mechanochemical signaling activities in a living cell. Sci Signal. 2008; 1:pl1. [PubMed: 18728305]
12. Taguchi K, Ishiuchi T, Takeichi M. Mechanosensitive EPLIN-dependent remodeling of adherens junctions regulates epithelial reshaping. J Cell Biol. 2011; 194:643–656. [PubMed: 21844208]
13. Huveneers S, Oldenburg J, Spanjaard E, van der Krogt G, Grigoriev I, Akhmanova A, Rehmann H, de Rooij J. Vinculin associates with endothelial VE-cadherin junctions to control force-dependent remodeling. J Cell Biol. 2012; 196:641–652. [PubMed: 22391038]
14. Thomas WA, Boscher C, Chu YS, Cuvelier D, Martinez-Rico C, Seddiki R, Heysch J, Ladoux B, Thiery JP, Mege RM, et al. Alpha-Catenin and Vinculin Cooperate to Promote High E-cadherin-based Adhesion Strength. J Biol Chem. 2013; 288:4957–4969. [PubMed: 23266828]
15. Twiss F, le Duc Q, vanderHorst S, Tabdili H, vanderKrogt G, Wang N, Rehmann H, Huveneers S, Leckband D, de Rooij J. Vinculin-dependent cadherin mechanosensing regulates efficient epithelial barrier formation. Biol Open. 2012 submitted.
16. Barry AK, Tabdili H, Muhamed I, Wu J, Shashikanth N, Gomez GA, Yap AS, Gottardi CJ, de Rooij J, Wang N, et al. Alpha-Catenin cytomechanics: role in cadherin-dependent adhesion and mechanotransduction. J Cell Sci. 2014; 127:1779–1791. [PubMed: 24522187]

17. Ladoux B, Anon E, Lambert M, Rabodzey A, Hersen P, Buguin A, Silberzan P, Mege RM. Strength dependence of cadherin-mediated adhesions. Biophys J. 2010; 98:534–542. [PubMed: 20159149]
18. Geiger B, Spatz JP, Bershadsky AD. Environmental sensing through focal adhesions. Nature Rev. 2009; 10:21–33.
19. Ozawa M, Hoschutzky H, Herrenknecht K, Kemler R. A possible new adhesive site in the cell-adhesion molecule uvomorulin. Mech Dev. 1990; 33:49–56. [PubMed: 1710917]
20. Maruthamuthu V, Sabass B, Schwarz US, Gardel ML. Cell-ECM traction force modulates endogenous tension at cell-cell contacts. Proc Natl Acad Sci U S A. 2011; 108:4708–4713. [PubMed: 21383129]
21. le Duc Q, Shi Q, Blonk I, Sonnenberg A, Wang N, Leckband D, de Rooij J. Vinculin potentiates E-cadherin mechanosensing and is recruited to actin-anchored sites within adherens junctions in a MyosinII dependent manner. J Cell Biol. 2010; 189:1107–1115. [PubMed: 20584916]
22. Drees F, Pokutta S, Yamada S, Nelson WJ, Weis WI. Alpha-catenin is a molecular switch that binds E-cadherin-beta-catenin and regulates actin-filament assembly. Cell. 2005; 123:903–915. [PubMed: 16325583]
23. Piljic A, de Diego I, Wilmanns M, Schultz C. Rapid development of genetically encoded FRET reporters. ACS Chemical Biology. 2011; 6:685–691. [PubMed: 21506563]
24. Sun Y, Wang X, Yuan S, Dang M, Li X, Zhang XC, Rao Z. An open conformation determined by a structural switch for 2A protease from coxsackievirus A16. Protein & Cell. 2013; 4:782–792. [PubMed: 24026848]
25. Tabdili H, Langer M, Shi Q, Poh Y-C, Wang N, Leckband D. Cadherin-dependent mechanotransduction depends on ligand identity but not affinity. J Cell Sci. 2012; 125:4362–4371. [PubMed: 22718345]
26. Weber GF, Bjerke MA, DeSimone DW. A mechanoresponsive cadherin-keratin complex directs polarized protrusive behavior and collective cell migration. Dev Cell. 2012; 22:104–115. [PubMed: 22169071]
27. Na S, Collin O, Chowdhury F, Tay B, Ouyang M, Wang Y, Wang N. Rapid signal transduction in living cells is a unique feature of mechanotransduction. Proc Natl Acad Sci U S A. 2008; 105:6626–6631. [PubMed: 18456839]
28. Benjamin JM, Kwiatkowski AV, Yang C, Korobova F, Pokutta S, Svitkina T, Weis WI, Nelson WJ. AlphaE-catenin regulates actin dynamics independently of cadherin-mediated cell-cell adhesion. J Cell Biol. 2010; 189:339–352. [PubMed: 20404114]
29. Collins C, Guilluy C, Welch C, O'Brien ET, Hahn K, Superfine R, Burridge K, Tzima E. Localized tensional forces on PECAM-1 elicit a global mechanotransduction response via the integrin-RhoA pathway. Curr Biol. 2012; 22:2087–2094. [PubMed: 23084990]
30. Yao M, Qiu W, Liu R, Efremov AK, Cong P, Seddiki R, Payre M, Lim CT, Ladoux B, Mege RM, et al. Force-dependent conformational switch of alpha-catenin controls vinculin binding. Nature Comm. 2014; 5:4525.
31. Desai R, Sarpal R, Ishiyama N, Pellikka M, Ikura M, Tepass U. Monomeric alpha-catenin links cadherin to the actin cytoskeleton. Nat Cell Biol. 2013; 15:261–273. [PubMed: 23417122]
32. Pappas DJ, Rimm DL. Direct interaction of the C-terminal domain of alpha-catenin and F-actin is necessary for stabilized cell-cell adhesion. Cell Commun Adhes. 2006; 13:151–170. [PubMed: 16798615]
33. Rangarajan ES, Izard T. Dimer asymmetry defines alpha-catenin interactions. Nat Struct Mol Biol. 2013; 20:188–193. [PubMed: 23292143]
34. Kwiatkowski AV, Maiden SL, Pokutta S, Choi HJ, Benjamin JM, Lynch AM, Nelson WJ, Weis WI, Hardin J. In vitro and in vivo reconstitution of the cadherin-catenin-actin complex from Caenorhabditis elegans. Proc Natl Acad Sci U S A. 2010; 107:14591–14596. [PubMed: 20689042]
35. Peng X, Cuff LE, Lawton CD, DeMali KA. Vinculin regulates cell-surface E-cadherin expression by binding to beta-catenin. J Cell Sci. 2011; 123:567–577. [PubMed: 20086044]
36. Ziegler WH, Liddington RC, Critchley DR. The structure and regulation of vinculin. Trends Cell Biol. 2006; 16:453–460. [PubMed: 16893648]

37. Peng X, Maiers JL, Choudhury D, Craig SW, DeMali KA. alpha-Catenin uses a novel mechanism to activate vinculin. J Biol Chem. 2012; 287:7728–7737. [PubMed: 22235119]

38. Vermeulen SJ, Bruyneel EA, Bracke ME, De Bruyne GK, Vennekens KM, Vleminckx KL, Berx GJ, van Roy FM, Mareel MM. Transition from the noninvasive to the invasive phenotype and loss of alpha-catenin in human colon cancer cells. Cancer Res. 1995; 55:4722–4728. [PubMed: 7553655]

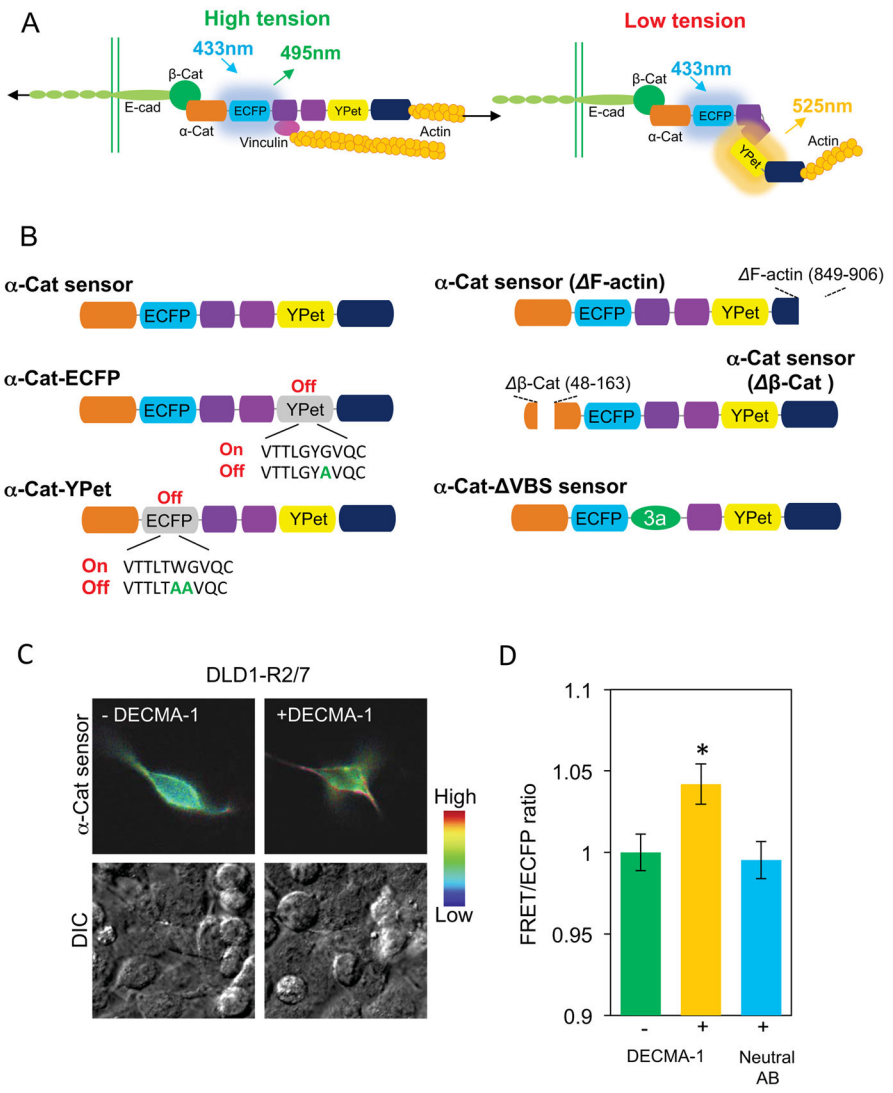

Figure 1. Design and characterization of the FRET-based α-catenin conformation sensor

(A) Schematic of the postulated mechanism underlying α-catenin tension sensing. In this mechanism, high tension between cadherin/catenin adhesive complexes and F-actin induces a conformational change that would separate ECFP and YPet, to reduce the FRET/ECFP ratio (left). Under low tension (for example, inactivated E-cadherin or actin disruption), the close fluorophores would increase the FRET/ECFP ratio (right). **(B)** α-catenin sensor and mutants used in this study. In the wild type sensor, two fluorescent proteins, ECFP and YPet were inserted within flexible linker regions flanking the central force-sensitive region (domains D2–D4, purple). The orange and dark blue domains are the β–catenin- (D1) and the F-actin-binding (D5) domains. Sensor variants include fluorophore mutants α–Cat-ECFP and α–Cat-YPet, truncation mutants lacking F-actin (ΔF-actin) or β–catenin (Δβ-Cat) binding regions, and the α–Cat-ΔVBS mutant lacking the vinculin-binding-site. **(C)** FRET/ECFP (top) and DIC (bottom) images of DLD1-R2/7 cells transfected with the sensor, before (left) and after (right) treatment with 50 μg/ml DECMA-1 antibody. **(F)** Bar graph quantifying the relative impact of blocking DECMA-1 and neutral antibody treatment on the

FRET/ECFP ratio at transfected DLD1-R2/7 cell junctions, compared to untreated cells (bar graph, n=43–61, *P<0.05). Error bars are the standard error of the mean (SEM).

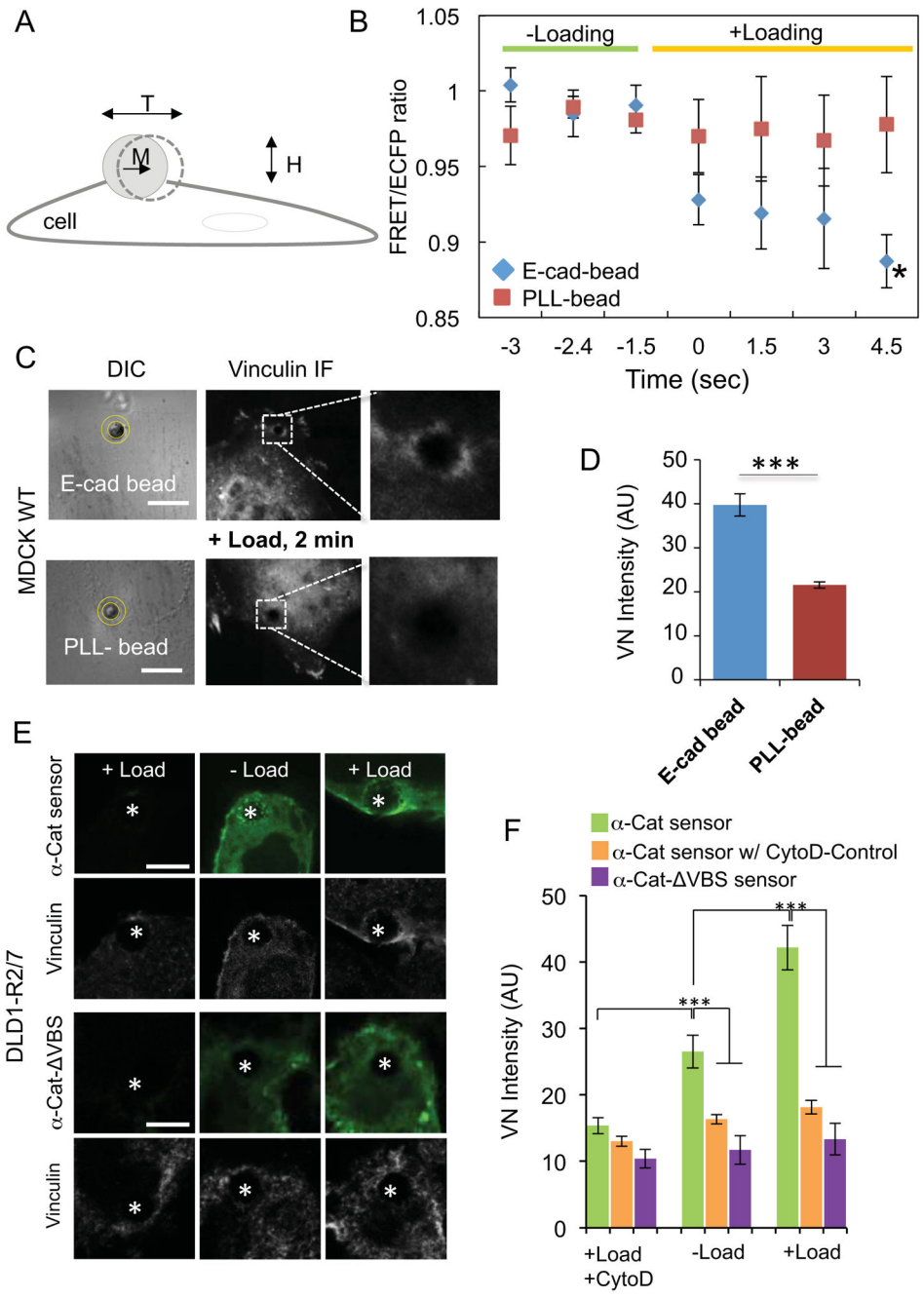

Figure 2. Acute mechanical perturbation of E-cadherin receptors triggers immediate α-catenin conformational switching and vinculin recruitment

(A) Schematic of the magnetic twisting cytometry (MTC) experiment. Ligand-coated, ferromagnetic beads with a magnetic moment (M) are subjected to an orthogonal, oscillating field (H), which generates a torque (T) on the bead. The torque causes bead displacement, the amplitude of which is proportional to the bead-cell junction viscoelasticity. **(B)** FRET/ECFP change in a region of interest (yellow circles, panel C) around the E-cadherin-Fc or PLL-coated beads bound to MDCK WT cells expressing the sensor (E-cadherin-Fc bead, n=8, versus control PLL-bead, n=4, *P<0.05). **(C)** DIC and vinculin immunofluorescence

images of MDCK WT cells after 2 min of twisting beads bound to the apical surfaces. Images on the right were cropped and enlarged from the boxed regions of the original images. The DIC images indicate the region of interest (ROI, yellow circles) used to quantify the distribution of vinculin at bead-cell junctions. Scale bar = 10 μm. **(D)** Bar graph comparing the average vinculin accumulation (arbitrary units, AU) at E-cadherin beads versus control PLL-beads on sensor-transfected MDCK WT cells, after 2min of loading (n=21–24, ***P<0.001). **(E)** Sensor (green) and vinculin (grey scale) distributions at E-cadherin beads on DLD1-R2/7 cells expressing the WT α–Cat sensor (top) or the α–Cat-ΔVBS sensor (bottom). The white asterisk denotes the bead position. Scale bars = 5 μm. Left panels are controls with non-transfected cells, after loading. The center and right panels show sensor and vinculin localization, before and after loading. **(F)** Bar graph comparing vinculin recruitment to E-cadherin beads on DLD1-R2/7 cells in panel E, with or without force loading (n=28–36, ***P<0.001). CytoD treatment significantly reduced vinculin recruitment to E-cadherin beads in cells expressing the WT α–Cat sensor (n=24–36). Error bars (B,D & F) indicate the SEM.

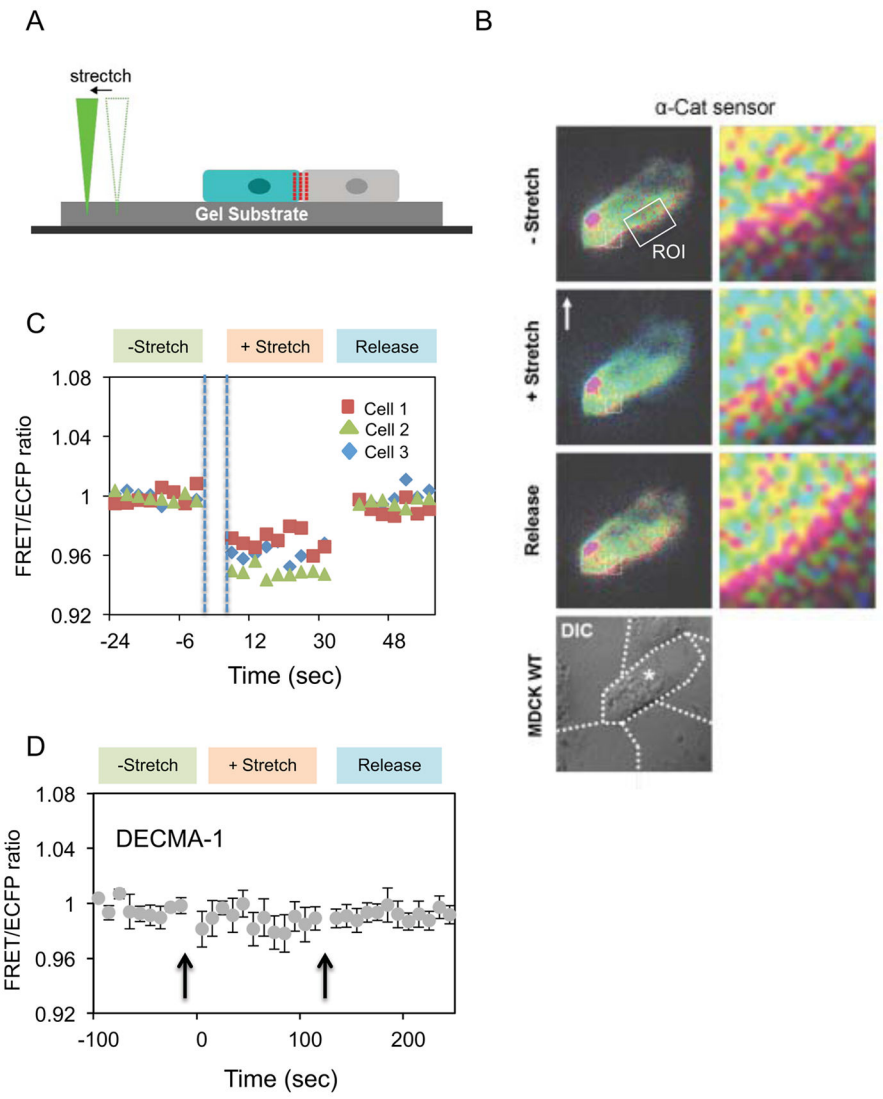

Figure 3. Exogneous mechanical stretch induces abrupt, reversible α-catenin conformation switching at intercellular junctions

(A) Schematic of the stretching device used to mechanically perturb MDCK WT cells seeded on PA gels (20 kPa) coated with fibronectin. **(B)** FRET/ECFP images monitored following substrate stretch and release by the probe, with the direction of the pull relative to the cell indicated by the white arrow. The box indicates the region of interest at the junction. The bright red spot in the FRET/ECFP image is a dust particle. **(C)** FRET/ECFP ratio versus time before, during, and after release of substrate strain. Data were obtained with MDCK WT cells transiently transfected with the sensor. Time points were taken with a 3s delay between nanoprobe stretch/release and fluorescence imaging. All three cells exhibited similar behavior following substrate stretch and release. **(D)** Effect of the E-cadherin blocking antibody DECMA-1 on the FRET/ECFP ratio versus time during stretch/release cycles. Error bars indicate the SEM.

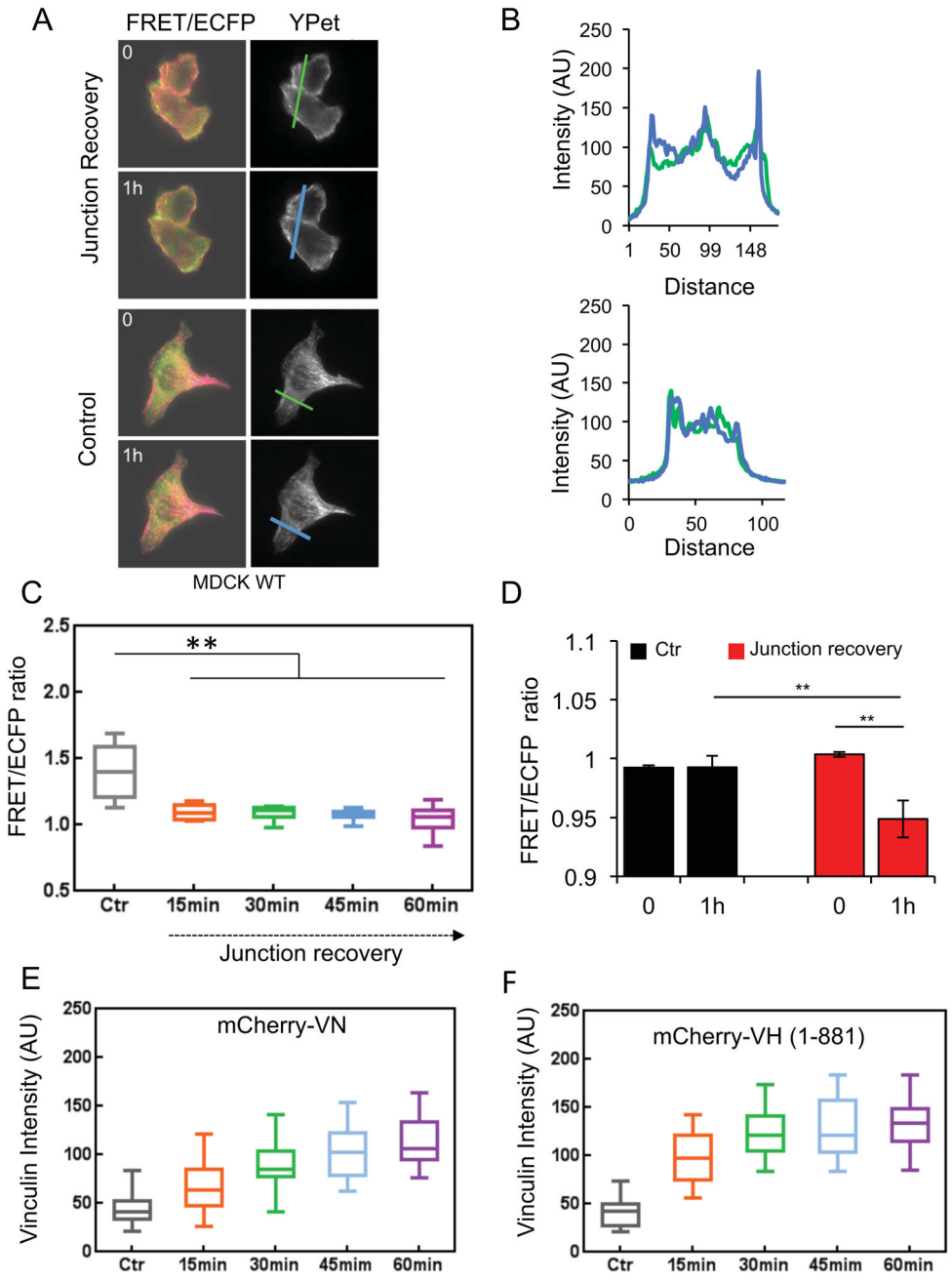

Figure 4. Dynamics of α–catenin conformation switching and vinculin recruitment during junction recovery following a calcium switch

A) FRET/ECFP and YPet fluorescence images initially and 1 hr after activating cadherin adhesive function with 2 mM Ca^{2+}. Images of unstimulated, control cells are in the lower panels. **(B)** Line-scan analyses of the YPet intensity at the indicated junctions (left) of Ca^{2+} treated (top panels) and control cells (bottom panels) during junction recovery. Line scans were at 0 hr (green line) and 1 hr (blue line). In treated cells (top), the decreased FRET/ECFP ratio coincides with an increase in total YPet intensity, due to sensor accumulation at the junctions. **(C)** FRET/ECFP ratio versus time after calcium addition (n=9–10). **(D)** Bar

graphs of the FRET/ECFP ratios before and 1 hr after Ca^{2+} addition (red bars), and in untreated control cells (black bars). After 1 hr, the decreased FRET/ECFP ratio indicates α-catenin conformation switching at re-annealing junctions (n=6, **P< 0.01). **(E)** Time dependence of the background-subtracted mCherry-VN fluorescence at ROIs at junctions, after calcium addition (n = 31–36). **(F)** Background-subtracted mCherry VH (1-881) fluorescence at junctions versus time after calcium addition, (n=31–35). In panels C–D, error bars indicate the SEM.